EBioMedicine 54 (2020) 102715

Contents lists available at ScienceDirect

EBioMedicine

journal homepage: www.elsevier.com/locate/ebiom

Research paper

# Targeted apoptosis of myofibroblasts by elesclomol inhibits hypertrophic scar formation

Yi Feng[a,b], Jun-Jie Wu[a], Zi-Li Sun[a,c], Si-Yu Liu[a,c], Ming-Li Zou[a,c], Zheng-Dong Yuan[a], Shun Yu[a,c,d], Guo-Zhong Lv[a,c,d,e], Feng-Lai Yuan[a,c,d,e,*]

[a] Department of Burns and Plastic Surgery, The Affiliated Hospital of Jiangnan University, Wuxi 214041, China
[b] Department of Pharmacology, Medical School, Yangzhou University, Yangzhou 225001, China
[c] Wuxi Clinical Medicine School of Integrated Chinese and Western Medicine, Nanjing University of Chinese Medicine, Wuxi 214041, China
[d] Department of Central Laboratory, The Third Hospital Affiliated to Nantong University, Wuxi, Jiangsu 214041, China
[e] Engineering Research Center of the Ministry of Education for Wound Repair Technology, Jiangnan University, Wuxi 214041, China

ARTICLE INFO

*Article History:*
Received 29 November 2019
Revised 27 February 2020
Accepted 28 February 2020
Available online xxx

*Keywords:*
Elesclomol
Hypertrophic scar
Apoptosis
Myofibroblasts
ROS

ABSTRACT

*Background:* Hypertrophic scar (HS) is characterized by the increased proliferation and decreased apoptosis of myofibroblasts. Myofibroblasts, the main effector cells for dermal fibrosis, develop from normal fibroblasts. Thus, the stimulation of myofibroblast apoptosis is a possible treatment for HS. We aimed to explore that whether over-activated myofibroblasts can be targeted for apoptosis by anticancer drug elesclomol.
*Methods:* 4′,6-diamidino-2-phenylindole staining, flow cytometry, western blotting, collagen gel contraction and immunofluorescence assays were applied to demonstrate the proapoptotic effect of elesclomol in scar derived myofibroblasts and TGF-$\beta$1 induced myofibroblasts. The therapeutic potential of elesclomol was investigated by establishing rabbit ear hypertrophic scar models.
*Findings:* Both 4′,6-diamidino-2-phenylindole staining and flow cytometry indicated that elesclomol targets myofibroblasts in vitro. Collagen gel contraction assay showed that elesclomol inhibited myofibroblast contractility. Flow cytometry and western blot analysis revealed that elesclomol resulted in excessive intracellular levels of reactive oxygen species(ROS), and caspase-3 and cytochrome c proteins. Moreover, compared with the control group, the elesclomol group had a significantly lower scar elevation index in vivo. Immunofluorescence assays for TUNEL and $\alpha$-smooth muscle actin indicated that elesclomol treatment increased the number of apoptotic myofibroblasts.
*Interpretation:* The above results indicate that elesclomol exerted a significant inhibitory effect on HS formation via targeted myofibroblast apoptosis associated with increased oxidative stress. Thus, elesclomol is a promising candidate drug for the treatment of myofibroblast-related diseases such as HS.


## 1. Introduction

Hypertrophic scar (HS) is a scar resulting from the excessive proliferation of dermal fibroblasts during wound healing, which leads to the overproduction of collagen and excessive deposition of fibroblast-derived extracellular matrix [1,2]. HS is a relatively common complication of deep burns, inflammatory reactions, and trauma, with reported incidence rates of 40% after surgery and as high as 91% after burns [3,4]. HSs are often painful, itchy, and associated with severe functional, cosmetic, and even psychological problems owing to complications such as anatomical deformities, stiffness, compression, and loss of joint mobility [5,6]. Numerous treatments for HS have been applied, such as surgical excision, pressure therapy, intralesional steroids, laser therapy, and cryotherapy [3,7,8], but the poor prognosis of HS are often unsatisfactory. Thus, new treatment strategies for HS are urgently required.

The main pathological change underlying HS formation is the development of numerous myofibroblasts (also known as activated fibroblasts) [9]; with HS progression, the persistence of myofibroblasts after wound healing may cause the fibroproliferative scar formation, which characterized by increased expression of $\alpha$-smooth muscle actin ($\alpha$-SMA), increased the ability of collagen synthesis [10,11]. Therefore, strategies that reduce fibroblast proliferation and increase fibroblast apoptosis might be effective for treating HS, and it is meaningful to study the myofibroblast apoptosis [12,13]. Moreover, emerging evidences have suggested that HS have some tumor-like properties due

Funding: Funding for this study was provided by the Natural Science Foundation of China (81770876), Natural Science Foundation of Jiangsu Province (Grant BK20191141).
* Corresponding author.
*E-mail address:* bjjq88@163.com (F.-L. Yuan).

https://doi.org/10.1016/j.ebiom.2020.102715

**Research in context**

*Evidence before this study*

The formation of hypertrophic scars is partially reflected in the excessive proliferation of myofibroblasts and the transformation of fibroblasts into myofibroblasts is an important target of anti-scar treatment. However, radical complete healing of HS is much more difficult to achieve. Elesclomol, an anticancer drug which has been proved to induce apoptosis in hyperproliferative cancer cells in recent studies. Thus, it is unknown whether the effects of eleclomol also can be applied in over-activated myofibroblasts in HS.

*Added value of this study*

In this study, we innovatively used a new anticancer drug eleclomol to explore the targeted apoptosis effect on myofibroblasts in HS. In vitro experiments, we proved that elesclomol increases the number of apoptotic $\alpha$-SMA(+) myofibroblasts and reduces human dermal myofibroblast phenotype and contractility. Furthermore, we identified the pro-apoptotic effects of elesclomol by increasing reactive oxygen levels. In vivo experiments, we demonstrated that elesclomol inhibits HS formation and promotes myofibroblast apoptosis in rabbit ears HS model.

*Implications of all the available evidence*

Targeting the apoptosis of myofibroblasts therefore be useful as a therapy to restrain progression of skin fibrosis. Our findings also suggest that elesclomol is potentially clinically effective and may become a promising strategy.

to its excessive and rapid cell overgrowth [14]. Indeed, in recent years, emerging evidence revealed that some anticancer agents have been used as off-label treatments for HS.

Elesclomol [STA-4783; *N*-malonyl-bis (*N′*-methyl-*N′*-thiobenzoylhydrazide] is an antitumor drug that was discovered using phenotype screening of small molecules and has potent proapoptotic activity, which is known as an apoptosis stimulant [15,16]. Elesclomol inhibits partial tumor-cell proliferation, induces tumor-cell apoptosis, and impedes tumor metastasis, it also targets various cancer cell types and enhances the role of paclitaxel in human tumor xenograft models. Elesclomol has received both fast track and orphan drug status from the U.S. Food and Drug Administration for the treatment of metastatic melanoma [17,18] and it is also being used in tumors such as non-small cell lung cancer, breast cancer and sarcoma [19,20]. Recently, elesclomol was shown to induce ROS production in tumor cells in vitro, leading to increased oxidative stress and apoptosis [21,22]. Considering its proapoptotic effects, we speculated that elesclomol may serve as a novel treatment for HS.

Therefore, we conducted the current study to determine whether elesclomol exhibits a proapoptotic effect on fibroblasts and myofibroblasts both in vitro and in vivo. Furthermore, we examined whether elesclomol treatment induced fibroblast and myofibroblast apoptosis by increasing ROS levels beyond a threshold that triggers cell apoptosis.

## 2. Materials and methods

### 2.1. Patients and ethics statement

We collected HS tissues from 6 patients (mean age, 30 years) who underwent surgical excision of HS in the Affiliated Hospital of Jiangnan University (Wuxi, China). The study purpose and the procedures involved were explained to the patients, who all consented in writing to the use of their resected tissue specimens in this study. The HS diagnosis was verified via routine pathological examination. Table 1 shows the details of the tissue specimens. The study protocols were approved by the ethics committee of the Affiliated Hospital of Jiangnan University.

### 2.2. Animals, reagents, and antibodies

New Zealand white rabbits, weighing 2.2−2.7 kg each, were purchased from the Hushan Experimental Animal Center (License no.: SCXK 2015-0004), Wuxi, China. The animal experiments were approved by the Experimental Animal Committee of Jiangnan University. Elesclomol (STA-4783) was obtained from Selleck Chemicals (Houston, TX, USA), dissolved in dimethyl sulfoxide (DMSO; Beyotime, Shanghai, China), and stored at −20 °C. Anti-$\beta$-actin antibody (ab16039) was purchased from Abcam (Cambridge, MA, USA). Cleaved caspase-3 (Asp175; 5A1E) rabbit mAb (#9664) was purchased from Cell Signaling Technology (Danvers, MA, USA). Caspase-3 rabbit antibody (19677-1-AP) was purchased from Proteintech (Chicago, IL, USA). 2,7-Dichlorofluorescin diacetate (DCFH-DA) was obtained from Sigma-Aldrich (D6883; St. Louis, MO, USA), and the Annexin V apoptosis-detection kit was obtained from Thermo Fisher Scientific (BMS500BT-100; Waltham, MA, USA). Recombinant human transforming growth factor (TGF)-$\beta$1 was purchased from PeproTech (#0212209; Rocky Hill, NJ, USA).

### 2.3. Rabbit ear HS model and treatment

Six 8-mm-wide full-thickness circular wounds were created on the ventral surface of each rabbit ear by removing the full layer of ear skin and perichondrium with an 8-mm biopsy punch. The wounds were washed with saline, and then, left exposed to air, with regular cleanings for the removal of secretions. The wounds crusted after 1 week, and the crusts were removed to expose the wounds again. HSs formed over the wounds approximately 3 weeks after the initial wounding. Any wound with infection or necrosis was excluded from the study. The rabbits were randomly divided into a control group, a vehicle group, and an elesclomol group. At 21 days after wounding, the wounds in the elesclomol group were injected with elesclomol dissolved in DMSO (10 mM, 50 $\mu$L), while those in the vehicle group were injected with 50 $\mu$L DMSO only. The wounds in the control group received no treatment. The injections were administered once every 2 days for a total of 7 times (14 days). At the end of this treatment period (35 days from wounding), the scar tissue in each group was collected for assays.

### 2.4. Cell extraction and culture

Fibroblasts were derived from normal human skin and pathological HS tissue collected during circumcision surgery and scar-removal surgery, respectively, with the consent of the patients. After being washing with phosphate-buffered saline (PBS), the scar tissues were incubated with collagenase type I (0.1 mg/mL; Sigma) at 37 °C for 5 h. The extracted fibroblasts and myofibroblasts were collected and cultured in Dulbecco-modified Eagle medium (DMEM; HyClone, South Logan, UT, USA) containing 10% fetal bovine serum (Gibco, Grand Island, NY, USA) at 37 °C in 5% $CO_2$. Cells at 70%−90% confluence were passaged (ratio, 1:2). All experiments were performed using cells between passages 3 and 5.

The cells were inoculated in a 24-well plate ($3 \times 10^4$ cells/well). After the cells had attached, they were starved by incubation in serum-free DMEM. After 12 h, 10 ng/mL TGF-$\beta$1 was added to each well for 48 h to induce the differentiation of the fibroblasts into myofibroblasts.

**Table 1**
Characteristics of human hypertrophic scars.

| No. | Age (y) | Sex | Biopsy site | Time after wounding | Type of wound | Wound size (length × width) |
|---|---|---|---|---|---|---|
| 1 | 37 | Male | Upper lip | 10 months | Surgical | 1.5 cm × 1.5 cm |
| 2 | 29 | Female | Clavicle | 1 year | Traumatic | 2 cm × 1.5 cm |
| 3 | 27 | Male | Left ulna | 1 year | Traumatic | 6 cm × 0.5 cm |
| 4 | 25 | Male | L2 vertebral body | 1 year | Traumatic | 4 cm × 3 cm |
| 5 | 31 | Female | Left foot | 2 year | Burn | 8.5 cm × 0.5 cm |
| 6 | 18 | Male | Right foot | 7 year | Traumatic | 5 cm × 0.5 cm |

### 2.5. Evaluation of treated scars

Hematoxylin and eosin (HE) staining and Mason trichrome staining were used to evaluate scar hypertrophy and collagen deposition, respectively. We used the scar elevation index (SEI), which is a reliable method to quantify scar formation [23]. The SEI is the ratio of the total height (H) of the wound tissue to the height (h) of the normal tissue under the scar: SEI = cross-sectional area of entire scar/cross-sectional area below the ridge. The above measurements were performed at a magnification of 100X, using Image-Pro-Plus v6.0. An SEI of 1 indicated normal wound healing without HS formation, while an SEI of $>1$ indicated HS. The SEI in each group was normalized relative to the vehicle group, which was arbitrarily assigned a value of 100%.

### 2.6. Immunofluorescence cell staining

Adherent fibroblasts in the 24-well plate were fixed with 4% paraformaldehyde for 15 min, permeabilized with 0.5% Triton-X100 for 20 min, and then blocked with goat serum for 30 min at 37 °C. The blocking solution was aspirated, and the cells were stained with anti-$\alpha$-SMA primary antibody (ab5694; Abcam) and incubated overnight at 4 °C. The next day, the cells were incubated with the coupled secondary antibody (#8889; Cell Signaling Technology) for 1 h at 37 °C. The cells were then washed with PBS, and 50 $\mu$L TUNEL test solution (TUNEL fluorescence-detection kit, Beyotime) was added to each well. The incubation was continued at 37 °C for 1 h in the dark, and the cells were washed again with PBS. DAPI was added to the cells at room temperature for 10 min. Finally, the stained cells were examined using an Olympus DP73 inverted photomicroscope (Olympus, Beijing, China). Negative controls were incubated with normal serum and the appropriate secondary antibodies. After the rabbit-ear sections were subjected to antigen retrieval and serum blocking, the subsequent steps were identical.

### 2.7. Flow cytometry for cell-apoptosis detection

Human fibroblasts were inoculated in culture flasks ($2 \times 10^5$ cells/mL). After the cells adhered to the flask, they were incubated with elesclomol (10 $\mu$M) for 24 h or an equal volume of DMEM (blank control). The cells were digested with 0.25% trypsin (Beyotime), washed once with PBS and once again with a binding buffer, and resuspended in the binding buffer at a density of $2 \times 10^6$ cells/mL. Fluorescein isothiocyanate (FITC)-conjugated annexin V (5 $\mu$L) was added to 100 $\mu$L of the cell suspension, after which it was incubated for 15 min at room temperature. The fibroblasts were washed again with the binding buffer and resuspended in 200 $\mu$L binding buffer, after which 5 $\mu$L propidium iodide (PI) staining solution was added to the cell suspension. Finally, the cell-apoptosis rate was detected using flow cytometry (BD FACSCalibur, San Jose, CA, USA).

### 2.8. Collagen gel contraction assay

Rat tail collagen was extracted according to the method described by Rittié [24] and purified; 5 × DMEM was added to the rat tail collagen. After the color of the mixture changed to golden yellow, 1 M NAOH was slowly added until the color changed to red, and then, 50,000 cells were inoculated in 200 $\mu$L collagen mixture, mixed, and added to a 24-well plate for 1 h. After collagen coagulation, elesclomol or TGF-$\beta$1 was added, according to the group. After 24 h and 48 h of culture, three-dimensional collagen was separated from the side walls and photographed to measure the gel contour. The ratio of the gel profile to the well profile was used as a measure of shrinkage strength.

### 2.9. Flow cytometry for intracellular ROS detection

Fibroblasts and myofibroblasts were seeded in 6-well plates ($2 \times 10^5$ cells/mL), and precultured in an incubator. After 24 h, the cells had attached to the plates; the culture solution was then removed, and the appropriate agent was added: DMEM containing 10 $\mu$M elesclomol in the elesclomol group and blank DMEM in the negative control group. After incubation for 24 h, the cells were removed, and the fluorescent reagent DCFH-DA (10 $\mu$M, 1 mL/well; Sigma-Aldrich) was added. After incubation for 24 h at 37 °C, the level of intracellular ROS was measured using flow cytometry.

### 2.10. Western blot analysis

The fibroblasts extracted from scar tissues were divided into 4 groups, and cultured for 24 h with DMEM supplemented with 2, 10, or 50 $\mu$M elesclomol. The control group was cultured with DMEM only. Total proteins were extracted from the fibroblasts by using the Tissue or Cell Total Protein Extraction Kit (Sangon, Shanghai, China), and the protein concentration was measured using the Enhanced BCA Protein Assay Kit (Beyotime). After being boiled with sodium dodecyl sulfate polyacrylamide gel electrophoresis (SDS-PAGE) Sample Loading Buffer (Beyotime) for 10 min, equal amounts of the protein extract were subjected to electrophoresis in 12% SDS-PAGE gels at 120 V for 1.5 h, and then transferred to PVDF membranes (Biosharp, Shanghai, China) at 200 mA for 60 min. The membranes were blocked with 5% nonfat milk in PBS with Tween and incubated overnight at 4 °C with one of the following primary antibodies: caspase-3 rabbit antibody (1:1000, 19677−1-AP; Proteintech), cleaved caspase-3 (1:1000, #9664; Cell Signaling Technology), cytochrome c (1:1000, #11940; Cell Signaling Technology), and anti-beta-actin antibody (1:1000, ab16039; Abcam). The membranes were then washed with PBST, and incubated with horseradish peroxidase-conjugated secondary antibody (1:10000, ZB-2301; ZBGB-BIO, Beijing, China) for 1 h. Signals were detected using ECL Western Blotting Substrate (Tanon, Shanghai, China), and protein bands were quantified by measuring the signal intensity using Image Pro-Plus v6.0.

### 2.11. Statistical analysis

Data are expressed as mean ± standard error of mean (SEM). Differences between two groups were analyzed using the Student *t*-test, and differences among three or more groups were analyzed using one-way analysis of variance and the post-hoc least significant difference test. We used SPSS for Windows v17 for the analyses. *P* values $<0.05$ were considered statistically significant.

## 3. Results

### 3.1. Elesclomol promotes in vitro apoptosis of HS-derived human myofibroblasts

Cell viability was assessed by a CCK-8. The skin-derived fibroblasts and scar-derived myofibroblasts were exposed to different concentrations of elesclomol (0.08, 0.4, 2, 10, 50, 250 $\mu$M) for 24 h. As the concentration of elesclomol increased, the inhibition rate obviously increased (Supplementary Figure S1). This method confirmed that elesclomol could inhibit the growth of scar-derived myofibroblasts. The concentration of elesclomol, which resulted in the inhibition rate >50%, was selected in the following experiments.

To evaluate the effect of elesclomol on the apoptosis of fibroblasts and myofibroblasts, we treated these cells with a serum-free medium (blank control) and elesclomol, stained them with FITC-annexin V and PI, and then passed them through a flow cytometer to monitor their fluorescent signals. The flow cytometry results indicated that elesclomol preferentially induced the apoptosis of $\alpha$-SMA(+) myofibroblasts derived from scar tissues as well as those induced by TGF-$\beta$1. In comparison, the apoptosis rate was unchanged in blank DMEM-treated cells and $\alpha$-SMA(-) fibroblasts. This finding suggests that elesclomol targets $\alpha$-SMA(+) myofibroblasts, which are often referred to as myofibroblasts (Fig. 1B–D). After 24 h of treatment, changes to the nuclear morphology of DAPI-stained cells were observed using fluorescence microscopy. Kernel size and roundness were used to indicate early and delayed cell damage [25]. The results revealed that $\alpha$-SMA(+) myofibroblasts derived from scar tissue and those induced by TGF-$\beta$1 had high rates of apoptosis at 24 h after the administration of elesclomol, with most cells showing corona-like zones around the nuclei, condensed nuclear chromatin, and the concentration of a small portion of chromatin. Furthermore, DAPI fluorescent labeling showed that elesclomol had no significant effect on the apoptosis rate of normal skin-derived $\alpha$-SMA(-) fibroblasts (Fig. 1E, F), which is consistent with the flow cytometry results. The above data indicate that elesclomol induced the targeted apoptosis of myofibroblasts derived from HSs in vitro.

### 3.2. Elesclomol regulates human dermal myofibroblast phenotype and contractility

F-actin and $\alpha$-SMA play key roles in skin fibrosis, and their expression levels correlate with the contractility of myofibroblasts. To examine the role of elesclomol in myofibroblast phenotype and contractility, we incubated $\alpha$-SMA(+) myofibroblasts with F-actin and $\alpha$-SMA, followed by treatment with elesclomol for 24 h. As seen in Fig. 2A and B, the number of F-actin- and $\alpha$-SMA-positive cells were significantly reduced when cells incubated with TGF-$\beta$1 were treated with elesclomol, suggesting that elesclomol inhibited the formation of the dermal myofibroblast phenotype. To further explore the functional implications of myofibroblast contraction, we performed a collagen gel contraction assay (Fig. 2C and D). Elesclomol remarkably suppressed the contraction of TGF-$\beta$1-induced fibroblasts in a fibroblast-populated collagen lattice from 24 to 48 h, when compared with the control cells, suggesting that elesclomol inhibited the contractility of human dermal myofibroblasts.

### 3.3. Elesclomol promotes myofibroblast apoptosis by increasing oxidative stress

Elesclomol shows potent antitumor activity against a broad spectrum of cancers; this activity is exerted via increasing ROS and oxidative stress to levels that are lethal to cells [21]. Flow cytometry showed that the average fluorescence intensity of the elesclomol-treated cells increased as the drug concentration increased, as compared with the negative-control cells (Fig. 3A, B).

During apoptosis, caspase 3 is activated, and the enzyme cleaved caspase-3, which catalyzes nearly all apoptotic proteolysis, is the key to promoting apoptosis. Thus, cleaved caspase-3 is considered a reliable marker of apoptotic cell death [26,27]. Western blot analysis revealed that elesclomol increased the levels of caspase-3, cleaved caspase-3, and cytochrome c protein in the scar-derived fibroblasts in a concentration-dependent manner, indicating that elesclomol activates an endogenous pathway that induces apoptosis in myofibroblasts (Fig. 3C, D).

### 3.4. Elesclomol inhibits HS formation in rabbit ears

To investigate the impact of elesclomol on HS formation, we established the rabbit ear HS model. We created 6 full-thickness circular wounds on the ventral surface of each ear (Fig. 4A). The wounds were observed on days 5 to 7, and scar hyperplasia peaked after approximately 21 days. As shown in Fig. 4C, the wound areas on the rabbit ears in the no-treatment and vehicle groups consisted of prominent skin tissue with a tough texture, light red bulges, and hard areas. In contrast, the wound areas in the elesclomol group (0.2 mg elesclomol per wound area) appeared flatter and softer with a near-normal color.

HE-stained sections of rabbit ear tissue collected 35 days after wounding showed numerous fibroblasts in the blank control and vehicle groups, along with abundant fibroblast proliferation and coarsely arranged collagen fibers (Fig. 4D). In contrast, the tissues from the elesclomol group were flatter and had a significantly smaller cross-sectional wound area. These findings were consistent with the overall wound appearance (Fig. 4C). In addition, we performed Masson's trichrome staining, which stained the collagen fibers blue, and the cells interspersed between the collagen fibers light gray. Masson stained images showed that, in the elesclomol group, the collagen fibers were arranged regularly and loosely, while in the blank-control and vehicle groups, the fibers were disordered, dense, and even formed spiral-like tangles (Fig. 4E). Analysis of the Masson-stained images showed that elesclomol treatment reduced the SEI (Fig. 4F), which is considered to be the most objective criterion for assessing scar formation [28,29].

### 3.5. elesclomol promotes myofibroblast apoptosis in rabbit ear HS

To evaluate the effect of elesclomol on apoptosis in HS tissue, we performed TUNEL color development on rabbit ear-tissue sections. The results showed that after 14 days of elesclomol injection, the area of positively stained nuclei was significantly larger in the elesclomol group than in the control group, indicating that elesclomol increased cell apoptosis in the scar tissue. In addition, the number of apoptotic fibroblasts per unit area was significantly larger in the elesclomol group than in the control groups (Fig. 5A, B).

HSs exhibit excessive myofibroblast proliferation, and these myofibroblasts show significantly higher expression of $\alpha$-SMA than do fibroblasts in normal dermis. To demonstrate the targeted effect of elesclomol on myofibroblasts, we examined the rabbit ear-tissue specimens by using double immunofluorescence staining for TUNEL and $\alpha$-SMA, a myofibroblast-specific marker. Colocalization of TUNEL-positive and $\alpha$-SMA-positive cells confirmed that these cells were myofibroblasts. After 14 days of treatment, the number of TUNEL-positive cells was significantly higher while the $\alpha$-SMA expression level was significantly lower in the elesclomol group than in the untreated and vehicle groups (Fig. 5C, D). These findings indicate that elesclomol treatment significantly promoted myofibroblast apoptosis in the rabbit ear tissues.

## 4. Discussion

Myofibroblasts evade apoptosis in response to pro-survival biomechanical and growth factor signals from the fibrotic microenvironment. The present study showed that elesclomol promoted the

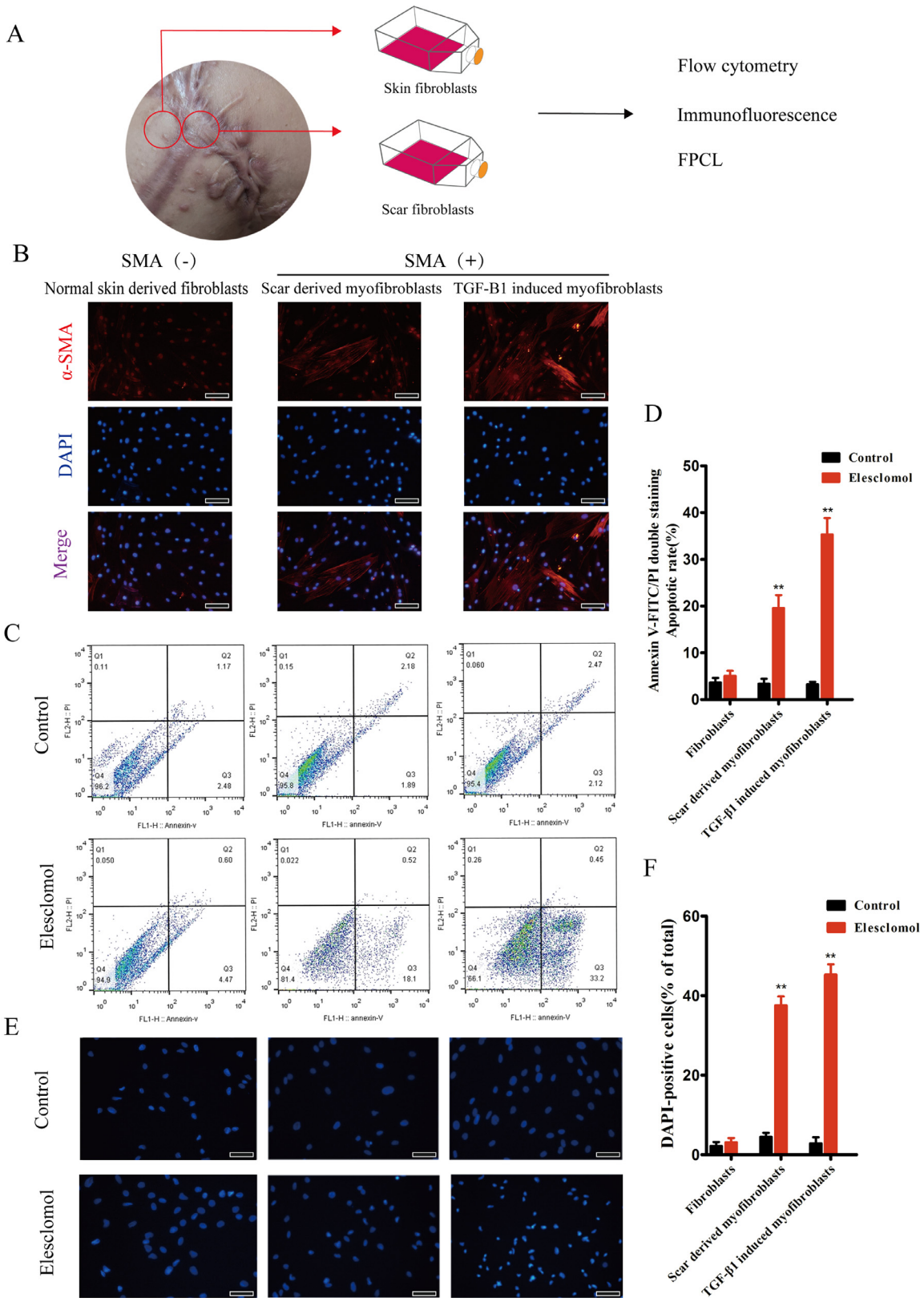


**Fig. 1.** Elesclomol increases the number of apoptotic $\alpha$-SMA(+) myofibroblasts in vitro. (A) Schematic diagram of different fibroblasts sources. (B) Normal skin-derived fibroblasts are $\alpha$-SMA negative, while scar-derived and TGF-induced myofibroblasts are $\alpha$-SMA positive. (C) Representative two-parameter flow cytometry dot plot. Cells double stained with annexin V-FITC and PI were subjected to flow cytometry. The total percentage of apoptotic cells is presented as the sum of the apoptotic-cell populations in the early and late stages. Serum-free medium served as a negative control. (D) Representative histogram showing a significant increase in apoptotic cells. (E) Representative immunofluorescence images of DAPI-stained fibroblasts showing higher apoptosis rates in HS-derived cells and those treated with 5 ng/mL TGF-$\beta$1 than in normal skin derived fibroblasts ($n$ = 6). Scale bar, 50 $\mu$m. (F) Quantification of DAPI-positive cells. $^{**}P < 0.01$ vs. control.

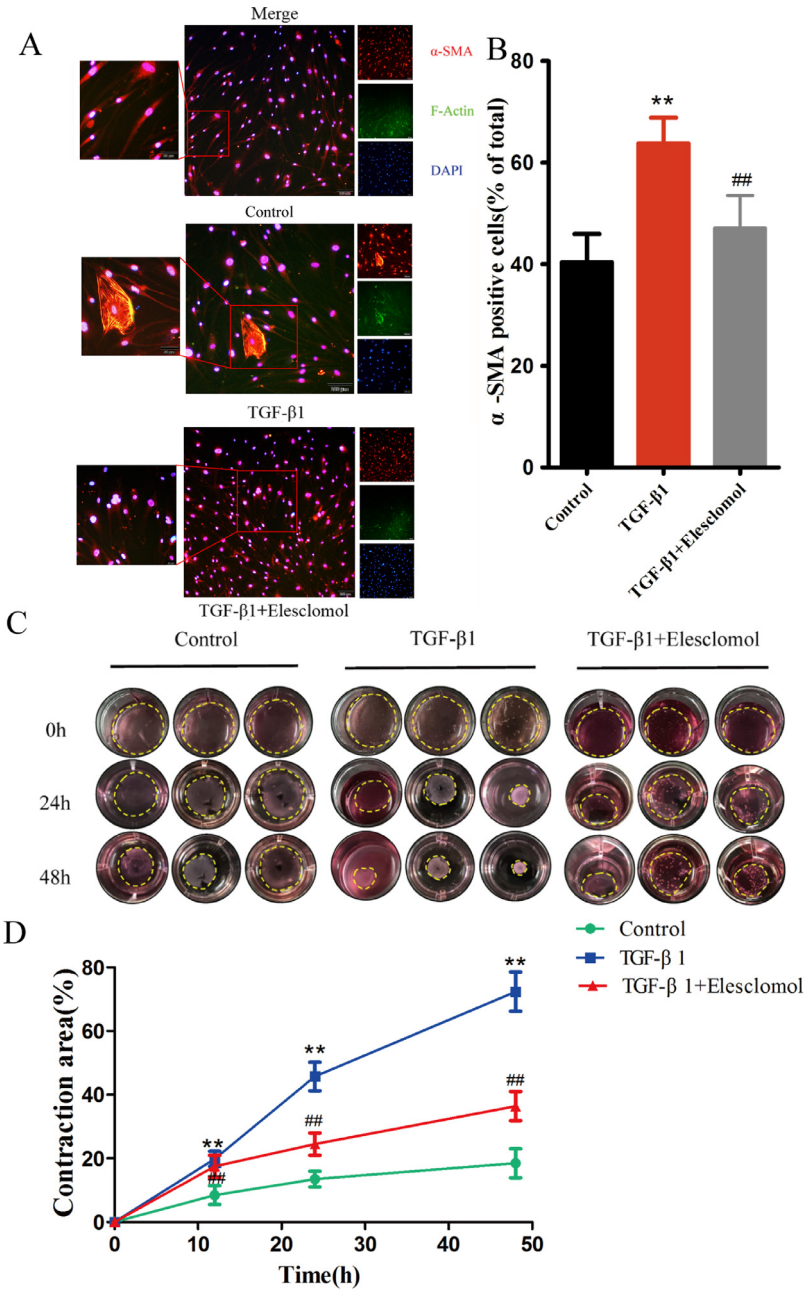


**Fig. 2.** Elesclomol regulates the contractility of myofibroblasts. (A) Representative double immunofluorescence images of apoptotic myofibroblasts incubated with F-actin (green) and $\alpha$-SMA antibody (red). The results show that the TGF-$\beta$1-induced upregulation of $\alpha$-SMA was inhibited by 10 $\mu$M elesclomol ($n$ = 9). Scale bar, 100 $\mu$m. (B) Quantification of $\alpha$-SMA-positive cells. (C) Effect of 10 $\mu$M elesclomol on the contractility of TGF-$\beta$1-induced fibroblasts. (D) The ratio of the gel outline to the well outline was taken as a measure of contraction strength. The results are expressed as mean ± SD ($n$ = 3). $^{**}P < 0.01$ vs. control, $\#\#P < 0.01$ vs. TGF-$\beta$1.

apoptosis of $\alpha$-SMA(+) myofibroblasts both in vitro and in vivo by increasing the intracellular ROS level and oxidative stress, which indicates the potential of elesclomol as a treatment for HS. To determine whether elesclomol could treat HS tissue without affecting the normal skin, we used primary dermal fibroblasts isolated from normal skin as well as hyperproliferative myofibroblasts isolated from HS tissue of patients. In the present study, DAPI staining showed no significant changes in the nuclei of fibroblasts derived from the normal skin after elesclomol administration, whereas at a high concentration of 50 $\mu$M elesclomol, the nuclei of scar-derived fibroblasts showed shrinkage or even lysis, resulting in apoptotic bodies. Similarly, flow cytometry showed that elesclomol effectively promoted the apoptosis of myofibroblasts, i.e., activated fibroblasts, but not of fibroblasts derived from normal skin. The above results confirmed that elesclomol can promote the apoptosis of myofibroblasts in a targeted manner.

TGF-$\beta$1 is an important factor inducing phenotypic changes in fibroblasts [30]. Based on the above experiments, we used TGF-$\beta$1 to induce the transformation of fibroblasts into myofibroblasts to determine the changes in the function and phenotype of myofibroblasts. Treatment of human skin fibroblasts with TGF-$\beta$1 resulted in the cells gaining a myofibroblast-like phenotype, as indicated by the significant upregulation of the myofibroblast marker $\alpha$-SMA and collagen gel contraction [31]. The collagen gel contraction assay has become a classic method for studying cell-induced extracellular matrix contraction in the field of mechanical biology; the extracellular matrix is crucial for wound healing [32]. In the collagen gel contraction test, 10 $\mu$M elesclomol significantly inhibited myofibroblast

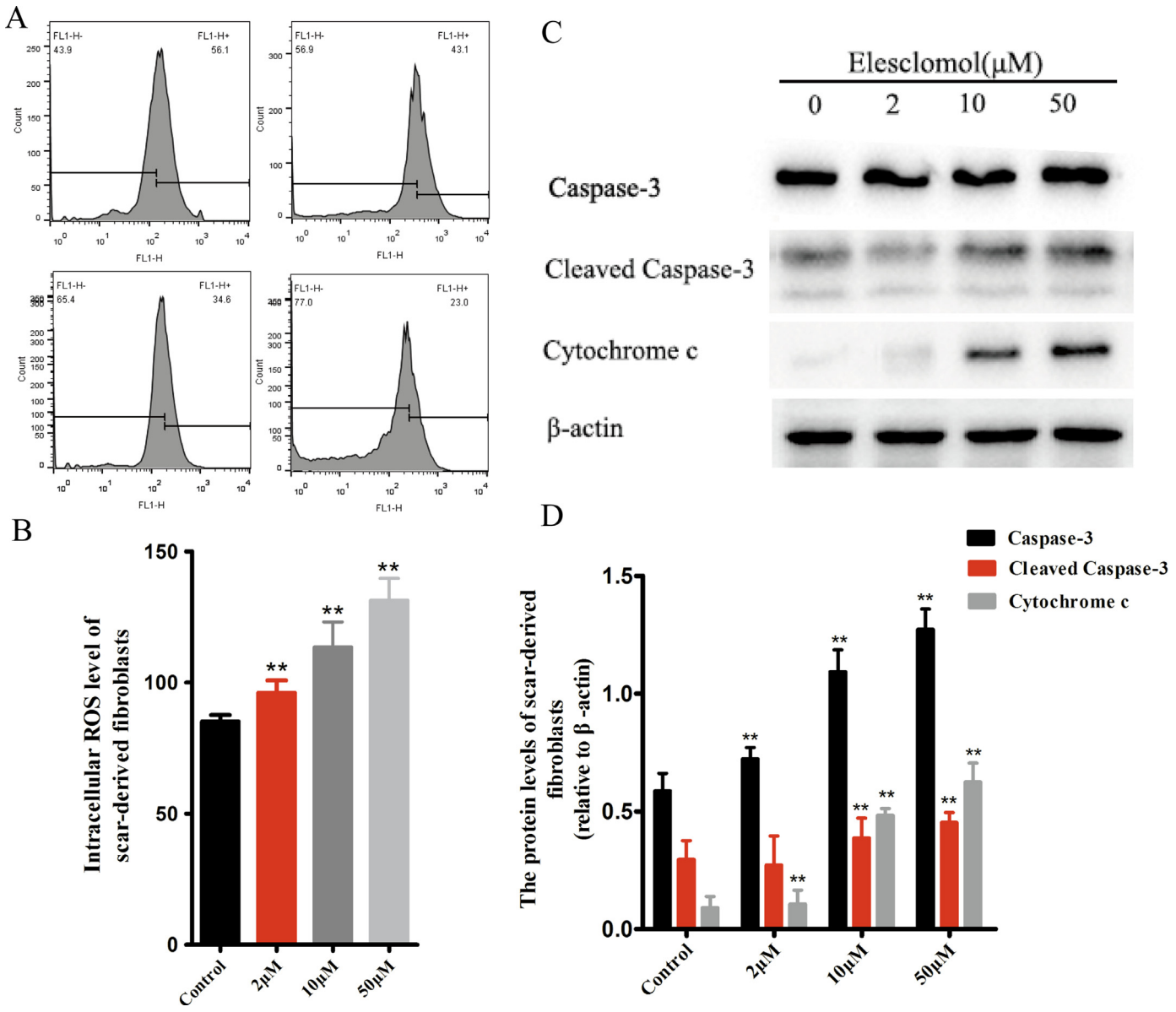


**Fig. 3.** Elesclomol promotes myofibroblast apoptosis by increasing intracellular ROS levels. (A) Elesclomol raises ROS levels in scar-derived fibroblasts in a concentration-dependent manner. Geo Mean data obtained using flow cytometry serve as a quantitative indicator of ROS. (B) Quantification of intracellular ROS levels at different elesclomol concentrations. (C) Western blot analysis of the levels of proteins that indicate cell apoptosis. Scar-derived fibroblasts were treated with blank DMEM or 2, 10, or 50 $\mu$M elesclomol for 24 h, and then, the total protein was extracted and subjected to western blot analysis. (D) Quantification of expression levels of caspase-3, cleaved caspase-3, and cytochrome c proteins. Data are expressed as mean ± SD ($n$ = 3/group). $^{**}P < 0.01$ vs. control.

differentiation as indicated by a marked decrease in gel contraction at 24 h after drug administration. Thus, elesclomol has the potential to inhibit the contractility of myofibroblast-like cells and block the differentiation of fibroblasts into myofibroblasts in a pathological setting.

Apoptosis occurs through internal and external pathways [33,34], and changes in mitochondrial ROS are mediated by internal pathways [35]. Mitochondrial dysfunction decreases ATP production and increases oxidative stress, resulting in cell apoptosis [36]. The relationship between ROS and hyperproliferative cells is well established, and elesclomol, a prooxidant drug, was discovered using cell-based phenotypic screening for the identification of apoptotic activity. Elesclomol exhibits an antitumor effect against melanoma cells and cells lacking electron transfer chain function, which confirms its role in the mitochondrial biological coherence [19,37]. Elesclomol has been reported to rescue mitochondrial absorption defects by increasing mitochondrial copper content and restoring cytochrome c oxidase activity via the regulation of oxidative stress [38–40]. Elesclomol can also chelate copper to form copper complexes through the redox cycle of metal ions, and greatly enhance oxidative stress in cancer cells [41]. Active oxygen detection was performed using DCFH-DA, fluorescent probe which itself has no fluorescence but can freely pass through cell membranes. Within the cell, it is hydrolyzed by esterase to form DCFH, which cannot penetrate cell membranes. The probe is thus loaded within cells. Intracellular ROS oxidize the non-fluorescent DCFH to the fluorescent DCF, and DCF fluorescence can measured to determine the level of intracellular ROS. We applied DCFH-DA probes to detect intracellular ROS, and the flow cytometry results clearly demonstrated that elesclomol promoted myofibroblast apoptosis by producing high levels of ROS in the cell organelles. Lagares et al. [42] found that myofibroblasts show increased expression of Bcl-xL, a member of the anti-apoptotic Bcl-2 family. ABT-263, a clinical anticancer drug, can reduce Bcl-xL levels and induce the self-destruction of hypertrophic myofibroblasts. After treatment with

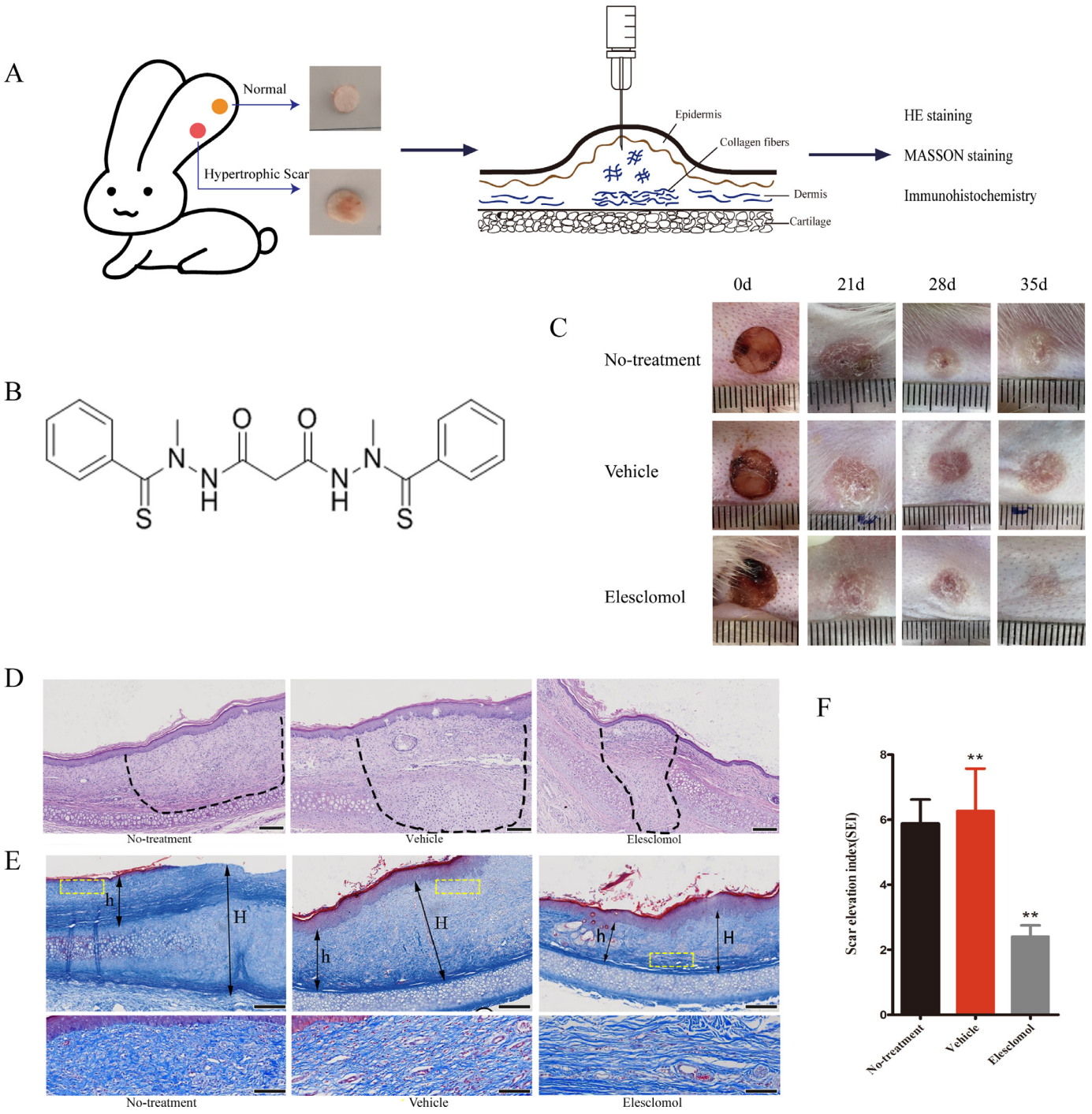


**Fig. 4.** Elesclomol inhibits HS formation in rabbit ears. (A) Schematic diagram of rabbit ear HS model. (B) Chemical structure of elesclomol ($C_{19}H_{20}N_4O_2S_2$; molecular weight, 400.52). (C) Photographs of the full-thickness skin wounds (wound diameter on day 0, 8 mm). (D) HE staining of scar tissue at 35 days after wounding. The dotted circles indicate the cross-sectional area of the HS. Scale bar, 200 $\mu$m. (E) Masson staining of scar tissue at 35 days after wounding. "H" indicates the scar thickness, while "h" indicates the normal skin thickness. Scale bar, 200 $\mu$m. Higher magnification images within the yellow dotted box show the difference of collagen fibers. Scale bar, 50 $\mu$m. (F) The scar elevation index was significantly lower in the elesclomol group than in the vehicle and untreated groups. Data are expressed as mean ± SD ($n$ = 6). $^{**}P < 0.01$ vs. control.

anticancer drugs, the activator originally bound to the anti-apoptotic receptor is replaced by the drug, allowing the proapoptotic protein Bax to initiate apoptosis in myofibroblasts. The above findings provide a possible explanation for the difference in the effects of elesclomol on normal dermal fibroblasts and scar-derived myofibroblasts. Whether or not elesclomol targets myofibroblasts via this mechanism will be the topic of our next study.

To explore the in vivo effects of elesclomol, we chose the widely accepted rabbit ear HS model. Although this model has some limitations related to the genetic predisposition and immune system of the animals [29], it is nevertheless useful to study the characteristics of HS formation, especially in the early stages. In this study, we created 6 wounds on each side of each rabbit ear, for a total of 48 wounds in each group. The incubation of human scar tissue with DMSO in vitro has proved that DMSO is involved in collagen fiber destruction. To eliminate the influence of DMSO [30], we set up a vehicle control group. After the regional injection, the thickness and cross-sectional area of the scar tissue were decreased, and the hard

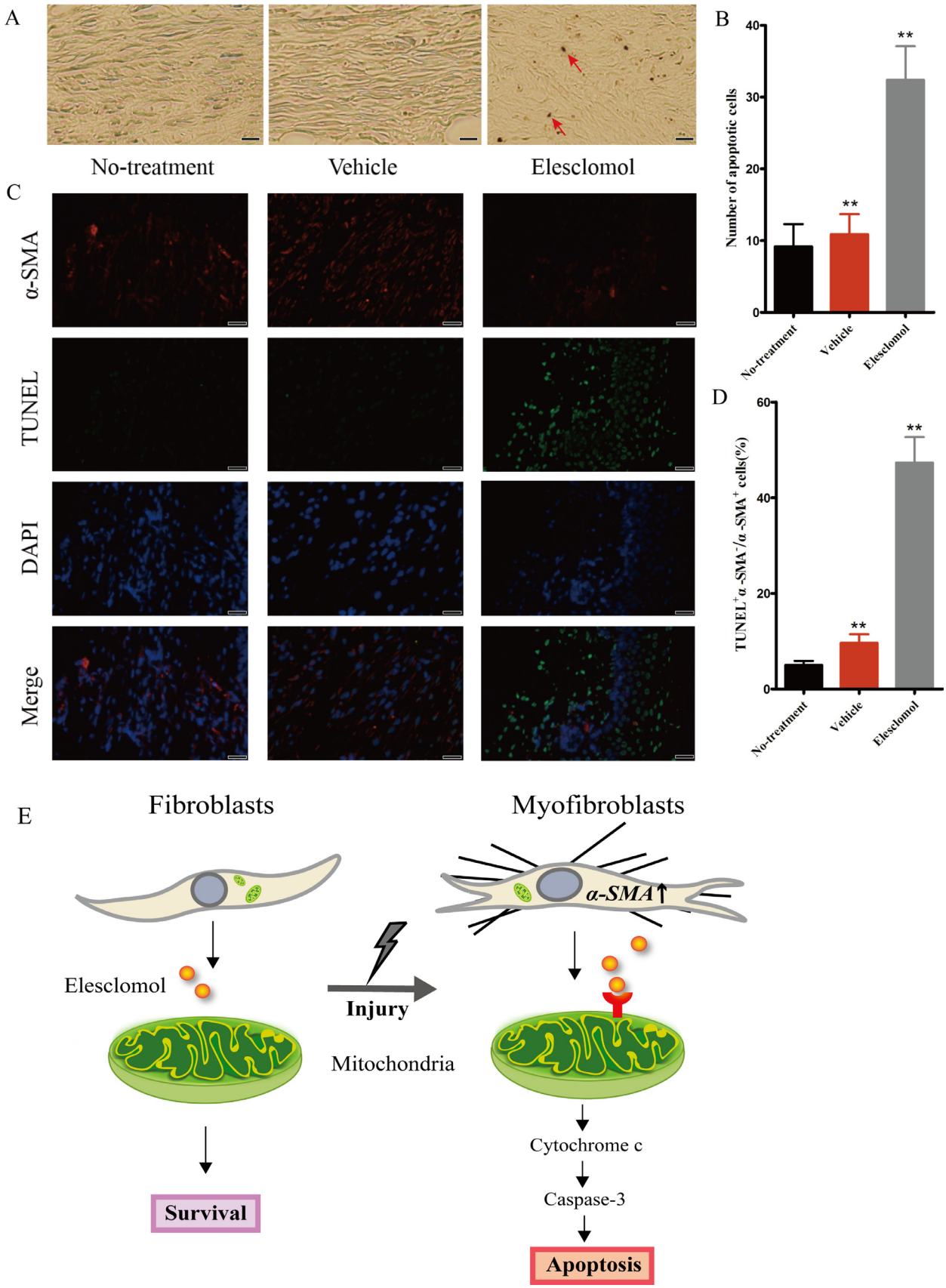


**Fig. 5.** Elesclomol increases the number of apoptotic scar-derived fibroblasts in vivo. (A) TUNEL-stained images taken after 14 days of treatment. The arrows indicate apoptotic cells ($n$ = 9). Scale bar, 50 $\mu$m. (B) Quantification of the percentage of TUNEL-positive cells. (C) Immunofluorescence images showing myofibroblast apoptosis in rabbit ears (TUNEL, green; DAPI, blue; anti-$\alpha$-SMA antibody, red). Scale bar, 50 $\mu$m. (D) Compared with the two control groups, the elesclomol group showed a significantly increased number of $\alpha$-SMA and TUNEL double-positive cells in rabbit ear scar tissue. Data are expressed as mean ± SD ($n$ = 7). $^{**}P < 0.01$ vs. the control groups. (E) Schematic diagram of elesclomol targeting apoptotic myofibroblasts in HSs.

scar tissue softened. Compared with the untreated group, the SEI of the hypertrophic scars formed in the vehicle group was slightly higher than that in the no-treatment group, which means that the wound scar was more serious; however, quantitative results showed that the SEI of the elesclomol group was significantly reduced with the vehicle group. The above results indicate that elesclomol is effective in treating HS in vivo. Elesclomol reduced the severity of hypertrophic scars, positively altered the appearance of the scars in the short term, and found no significant metabolic or laboratory abnormalities. In the model used, the chosen concentration of the drug proved to be safe and effective, with no evidence of systemic or local side effects.

To investigate the possibility of inducing HS by inducing fibroblast apoptosis, we performed TUNEL chromogenic assays of rabbit ear-tissue sections to determine whether elesclomol increased the number of apoptotic cells in HSs. To confirm that the apoptotic cells within the scar tissues were hyperproliferative myofibroblasts, we performed immunofluorescence double labeling experiments on rabbit ear sections. Several studies have shown high $\alpha$-SMA expression in scar-derived myofibroblasts as well as TGF-$\beta$1-induced myofibroblasts. In our fluorescence-stained images, the colocalization of $\alpha$-SMA and TUNEL demonstrated that elesclomol promotes the in vivo apoptosis of activated myofibroblasts in HSs.

In this study, our normal skin-derived fibroblasts were from normal peripheral skin near scar tissue, and SMA(+) myofibroblasts were from patient samples with different clinical characteristics. In order to reduce the experimental variability caused by sample differences, we performed DAPI staining on 6 cases of myofibroblasts from different sources. The results showed that there was no significant difference in apoptosis between different samples after administration and repeated experiments proved statistical significance (Supplementary Fig. S2), increasing the reliability of the experiment. However, the clinical sample size of scar patients is indeed a deficiency in our research and we will expand the sample size and conduct more rigorous research in the future. In our study, we also found that not only the escape of apoptosis of fibroblasts, but also macrophages and epithelial-mesenchymal transitions play an important role in scar formation [43,44], which provides a good direction for subsequent research.

In summary, the identification of new drug targets and the formulation of novel therapeutic strategies to prevent HS formation requires the investigation of how to properly initiate the apoptosis of myofibroblasts. This study found that elesclomol increases intracellular ROS levels to promote myofibroblast apoptosis and may prevent HS formation by disrupting the mitochondrial redox balance. In addition, our findings suggest that elesclomol could reverse tissue fibrosis. Considering the above findings, we conclude that elesclomol is a possible treatment for HS.

We also found that in addition to the fibrosis of the skin, which is related to the escape of fibroblasts from apoptosis, macrophages and epithelial-mesenchymal transitions have also played a significant role.

## Declaration of Competing Interest

The authors declare no competing interests with relevance to this study.

## Supplementary materials

Supplementary material associated with this article can be found in the online version at doi:10.1016/j.ebiom.2020.102715.

## References

[1] Sidgwick GP, Bayat A. Extracellular matrix molecules implicated in hypertrophic and keloid scarring. J Eur Acad Dermatol Venereol 2012;26(2):141–52.
[2] Lian N, Li T. Growth factor pathways in hypertrophic scars: molecular pathogenesis and therapeutic implications. Biomed Pharmacother 2016;84:42–50.
[3] Gauglitz GG, et al. Hypertrophic scarring and keloids: pathomechanisms and current and emerging treatment strategies. Mol Med 2011;17(1–2):113–25.
[4] Bao Y, et al. Comparative efficacy and safety of common therapies in keloids and hypertrophic scars: a systematic review and meta-analysis. Aesthetic Plast Surg 2019.
[5] Berman B, Maderal A, Raphael B. Keloids and hypertrophic scars: pathophysiology, classification, and treatment. Dermatol Surg 2017;43(Suppl 1):S3–S18.
[6] Brown BC, et al. The hidden cost of skin scars: quality of life after skin scarring. J Plast Reconstr Aesthet Surg 2008;61(9):1049–58.
[7] Del Toro D, Dedhia R, Tollefson TT. Advances in scar management: prevention and management of hypertrophic scars and keloids. Curr Opin Otolaryngol Head Neck Surg 2016;24(4):322–9.
[8] Benzaquen M, Collet-Villette AM, Delaporte E. Combined treatment of hypertrophic and keloid scars with intra-lesional injection of corticosteroids and laser-assisted corticosteroid delivery. Dermatol Ther 2019.
[9] Hinz B. The role of myofibroblasts in wound healing. Curr Res Transl Med 2016;64(4):171–7.
[10] Chen R, et al. Focal adhesion kinase (FAK) siRNA inhibits human hypertrophic scar by suppressing integrin alpha. TGF-beta and alpha-SMA. Cell Biol Int 2014;38(7):803–8.
[11] Gras C, et al. miR-145 contributes to hypertrophic scarring of the skin by inducing myofibroblast activity. Mol Med 2015;21:296–304.
[12] Darby IA, et al. The myofibroblast, a key cell in normal and pathological tissue repair. Cell Mol Life Sci 2016;73(6):1145–57.
[13] Yuan Q, Tan RJ, Liu Y. Myofibroblast in kidney fibrosis: origin, activation, and regulation. Adv Exp Med Biol 2019;1165:253–83.
[14] Han T, Lin DF, Jiang H. Wound natural healing in treatment of tumor-like hypertrophic scar. An Bras Dermatol 2017;92(4):474–7.
[15] Chen S, et al. Syntheses and antitumor activities of N'1,N'3-dialkyl-N'1,N'3-di-(alkylcarbonothioyl) malonohydrazide: the discovery of elesclomol. Bioorg Med Chem Lett 2013;23(18):5070–6.
[16] Albayrak G, et al. The outcomes of an impaired powerhouse in kras mutant lung adenocarcinoma cells by elesclomol. J Cell Biochem 2019;120(6):10564–71.
[17] Barbi de Moura M, et al. Mitochondrial respiration–an important therapeutic target in melanoma. PLoS One 2012;7(8):e40690.
[18] O'Day SJ, et al. Final results of phase III symmetry study: randomized, double-blind trial of elesclomol plus paclitaxel versus paclitaxel alone as treatment for chemotherapy-naive patients with advanced melanoma. J Clin Oncol 2013;31(9):1211–8.
[19] Gehrmann M, evaluation Drug. STA-4783–enhancing taxane efficacy by induction of HSP70. Curr Opin Investig Drugs 2006;7(6):574–80.
[20] Qu Y, et al. Elesclomol, counteracted by AKT survival signaling, enhances the apoptotic effect of chemotherapy drugs in breast cancer cells. Breast Cancer Res Treat 2010;121(2):311–21.
[21] Ren YJ, et al. Silencing of NAC1 expression induces cancer cells oxidative stress in hypoxia and potentiates the therapeutic activity of elesclomol. Front Pharmacol 2017;8:804.
[22] Kirshner JR, et al. Elesclomol induces cancer cell apoptosis through oxidative stress. Mol Cancer Ther 2008;7(8):2319–27.
[23] Morris DE, et al. Acute and chronic animal models for excessive dermal scarring: quantitative studies. Plast Reconstr Surg 1997;100(3):674–81.
[24] Rittie L. Type I collagen purification from rat tail tendons. Methods Mol Biol 2017;1627:287–308.
[25] Daniel B, DeCoster MA. Quantification of sPLA2-induced early and late apoptosis changes in neuronal cell cultures using combined tunel and dapi staining. Brain Res Brain Res Protoc 2004;13(3):144–50.
[26] Dolka I, Krol M, Sapierzynski R. Evaluation of apoptosis-associated protein (Bcl-2, Bax, cleaved caspase-3 and p53) expression in canine mammary tumors: an immunohistochemical and prognostic study. Res Vet Sci 2016;105:124–33.
[27] Crowley LC, Waterhouse NJ. Detecting cleaved caspase-3 in apoptotic cells by flow cytometry. Cold Spring Harb Protoc 2016;2016(11).
[28] Saulis AS, Mogford JH, Mustoe TA. Effect of mederma on hypertrophic scarring in the rabbit ear model. Plast Reconstr Surg 2002;110(1):177–83 discussion 184-6.
[29] Tandara AA, Mustoe TA. The role of the epidermis in the control of scarring: evidence for mechanism of action for silicone gel. J Plast Reconstr Aesthet Surg 2008;61(10):1219–25.
[30] Fang X, et al. Smad interacting protein 1 influences transforming growth factor-beta1/Smad signaling in extracellular matrix protein production and hypertrophic scar formation. J Mol Histol 2019.
[31] Manetti M, et al. Systemic sclerosis serum steers the differentiation of adipose-derived stem cells toward profibrotic myofibroblasts: pathophysiologic implications. J Clin Med 2019;8(8).
[32] Zhang T, et al. Investigating fibroblast-induced collagen gel contraction using a dynamic microscale platform. Front Bioeng Biotechnol 2019;7:196.
[33] Fulda S, Debatin KM. Extrinsic versus intrinsic apoptosis pathways in anticancer chemotherapy. Oncogene 2006;25(34):4798–811.
[34] Yang PY, et al. Norcantharidin induces apoptosis in human prostate cancer cells through both intrinsic and extrinsic pathways. Pharmacol Rep 2016;68(5):874–80.
[35] Yee C, Yang W, Hekimi S. The intrinsic apoptosis pathway mediates the pro-longevity response to mitochondrial ROS in C. elegans. Cell 2014;157(4):897–909.
[36] Greco V, et al. Crosstalk between oxidative stress and mitochondrial damage: focus on amyotrophic lateral sclerosis. Adv Exp Med Biol 2019;1158:71–82.

[37] Blackman RK, et al. Mitochondrial electron transport is the cellular target of the oncology drug elesclomol. PLoS ONE 2012;7(1):e29798.
[38] Gorrini C, Harris IS, Mak TW. Modulation of oxidative stress as an anticancer strategy. Nat Rev Drug Discov 2013;12(12):931–47.
[39] Kovacic P, Somanathan R. Recent developments in the mechanism of anticancer agents based on electron transfer, reactive oxygen species and oxidative stress. Anticancer Agents Med Chem 2011;11(7):658–68.
[40] Soma S, et al. Elesclomol restores mitochondrial function in genetic models of copper deficiency. Proc Natl Acad Sci U S A 2018;115(32):8161–6.
[41] Ngwane AH, et al. The evaluation of the anti-cancer drug elesclomol that forms a redox-active copper chelate as a potential anti-tubercular drug. IUBMB Life 2019;71(5):532–8.
[42] Lagares D, et al. Targeted apoptosis of myofibroblasts with the BH3 mimetic ABT-263 reverses established fibrosis. Sci Transl Med 2017;9(420).
[43] Feng Y, et al. Direct and indirect roles of macrophages in hypertrophic scar formation. Front Physiol 2019;10:1101.
[44] Yuan FL, et al. Epithelial-mesenchymal transition in the formation of hypertrophic scars and keloids. J Cell Physiol 2019;234(12):21662–9.